JOURNAL OF MATERIALS SCIENCE 10 (1975) 1375–1380

Creep of hot-pressed silicon nitride

SALAH UD DIN, PATRICK S. NICHOLSON
Department of Metallurgy and Materials Science, McMaster University, Hamilton, Ontario, Canada

Creep tests were undertaken on hot-pressed silicon nitride in the temperature range 1200 to 1400° C. The activation energy for creep was determined to be 140 kcal mol^{-1} and the stress exponent of creep rate was 1.7. The creep behaviour is ascribed to grain-boundary sliding accommodated by void deformation at triple points and by limited local plastic deformation. Electron microscopic evidence supporting this mechanism is presented.

1. Introduction

In recent years there has been considerable interest in hot-pressed silicon nitride because of its high strength. It has emerged as a prime candidate material for high efficiency gas turbines, and its creep behaviour is an essential design parameter.

Little or no creep data have been reported in the open literature on silicon nitride. In 1961 the creep characteristics of a low-strength material were studied by Glenny and Taylor [1], and Stokes *et al.* [2] made passing mention of the relative creep resistance of high- and low-strength silicon nitride materials in 1972. More recently, tensile and bend data generated by Westinghouse [3] have become available.

Creep of materials at high temperatures and low stresses can generally be divided into three creep-rate regimes. The initial deformation is rapid (stage I), and the creep rate subsequently decreases until the second stage (II) is reached, wherein the creep rate remains constant. Finally, in stage III, the creep rate increases again, producing cracks followed by failure. Most ceramics show the first two stages. This work was undertaken to investigate stage II or "steady state" creep of hot-pressed* silicon nitride and the microstructural changes associated therewith.

2. Experimental

2.1. Material characterization

The Si_3N_4 material was characterized by spectrographic analysis, bulk density measurements, grain size determinations and X-ray analysis. Samples for spectrographic analysis were ground in a silicon carbide mortar and pestle and dissolved in HF.

Spectrographic analysis revealed that the material was 97% silicon nitride. The major impurities were Ca (0.04 wt %), Mg (0.7 wt %), Fe (0.4 wt %), and Al (0.4 wt %). The density was found to be 98% of the theoretical value. Sections for grain size determination were mounted in plastic and rough polished with 400 grit diamond. Final polishing was undertaken on 0.25 μm diamond. After polishing, the samples were removed from the mount and etched in a mixture of HF, HNO_3, and H_2O_2 (1:1:3) at 80° C for 15 min. Shadowed replicas of the etched surface, made by the two-stage carbon replica technique, were examined in the electron microscope and grain sizes determined by the intercept method. About 85% of grains were equi-axed with diameter in the range 0.5 to 2 μm. The remainder were elongated with lengths in the range 1 to 5 μm large. X-ray diffraction showed that the β and α phases of silicon nitride were present. The energy-dispersive X-ray analysis technique was used to identify the intergranular glassy phase. It was found to be a compound of Mg, Ca, and Fe silicates.

2.2. Creep testing

All specimens were taken from a single hot-pressed billet to eliminate variables such as different chemical compositions and thermal history. The material was received in the form of $(1\frac{1}{4} \times \frac{1}{4} \times \frac{1}{4})$ in. bars.

Creep tests were conducted in four-point bending with silicon carbide knife edges and a

*Norton H.S. 130 Si_3N_4.

© *1975 Chapman and Hall Ltd.*

TABLE I

Specimen	Temperature	Stress (10^3 psi)	Strain after 80 h ϵ (%)	Steady state strain-rate $\dot{\epsilon}$ (h^{-1})
1	1260	8	0.16	3.8×10^{-6}
2	1260	10	0.20	0.6×10^{-5}
3	1260	15	0.41	1.25×10^{-5}
4	1260	20	0.63	2.00×10^{-5}
5	1300	10	0.86	1.6×10^{-5}
6	1300	15	1.02	2.8×10^{-5}
7	1300	20	1.24	4.5×10^{-5}
8	1350	10	1.18	6.5×10^{-5}
9	1350	15	1.47	1.5×10^{-4}
10	1350	20	1.80	2.5×10^{-4}
11	1400	10	1.55	2.1×10^{-4}
12	1400	15	1.82	4.5×10^{-4}
13	1400	20	2.1	5.8×10^{-4}

templet was used to centrally locate the samples. The desired load was applied by lowering appropriate slotted weights on to a load plate located on top of the sample loading column. Counter weights were used to balance the load-free column weight. A silicon carbide clamshell furnace was used to heat the sample to 1400 ± 5°C and a Pt/Pt–Rh thermocouple measured the specimen temperature. Samples were creep tested between 1200 and 1400°C at stresses between 8000 and 25 000 psi*. Maximum deformation was limited to about 3.0% and an LVDT utilized to monitor the creep deflection. The LVDT was mounted rigidly under the load plate.

A series of isothermal creep tests was undertaken for times up to 250 h (standard creep tests). In addition, individual specimens were creep tested by (a) stress cycling at constant temperature and (b) temperature cycling wherein the stress was held constant and the temperature changed incrementally. The former was used to evaluate the stress exponent of the creep rate and the latter to determine the activation energy for the creep process.

2.3. Electron microscopy

Samples for the electron microscopic analysis were taken from the tension edge of crept specimens. The first step involved the production of a geological thin section by grinding to 20 μm on a diamond wheel. The material was then ion-thinned until a small perforation was observed in the centre of the foil. A graphite film was evaporated onto the specimen before introduction into the transmission electron microscope.

3. Results

Creep data for the specimens tested are summarized in Table I. Typical standard creep curves at 1260 and 1300°C at a stress of 10 000 psi are shown in Fig. 1. The regimes of creep are readily distinguishable. The transients in all the creep tests were quite long (40 to 50 h) and, therefore, long-time tests (up to 250 h) were conducted.

The outer fibre stress and strain in bending specimens were calculated using the Timoshenko [4] elastic equations. The use of elastic equations for the evaluation of the plastic strain is questionable but it has been shown in a previous study [5] that for low plastic strains up to 3%, the elastic equations are valid.

Fig. 2 shows the log-log plot of steady state creep rate versus stress. The relationship between the two is given by the empirical law:

$$\dot{\epsilon} = A e^{-E/RT} \sigma^n \qquad (1)$$

where E is the activation energy.

From the slope of these plots, the stress exponent (n) of the creep rate was determined and is given in Table II. The exponent was also found by changing the stress level during a test and using Equation 1. The result of a stress change experiment is illustrated in Fig. 3.

The activation energy for the creep process was also determined in two ways, i.e. constant stress,

*10^3 psi ≡ 6.89 N mm^{-2}

TABLE II

Activation energy (kcal mol^{-1})			Stress exponent	
Temperature change (°C)	Temperature cycling experiment	Arrhenius plot	Stress change experiment	Arrhenius plot
1300–1350	140 ± 2	135 ± 2	1.70 ± 0.05	1.75 ± 0.02
1350–1400	144 ± 2	138 ± 2		

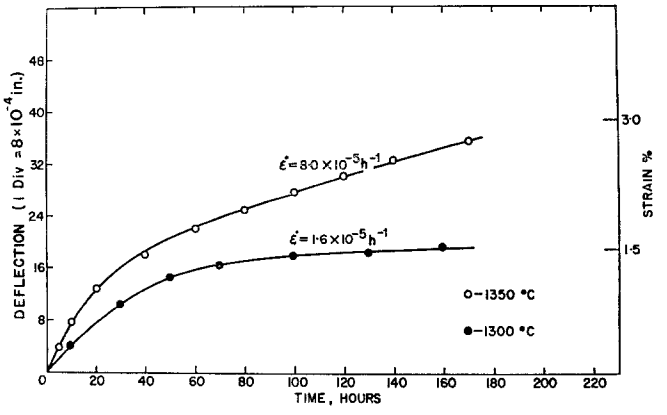

Figure 1 Strain-time curves.

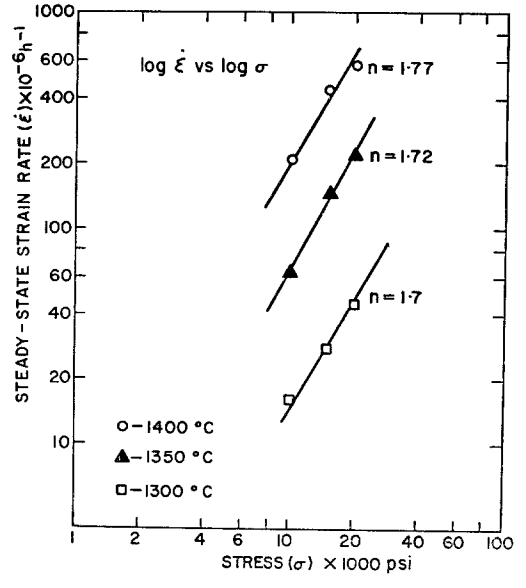

Figure 2 Steady state strain-rate as a function of stress.

temperature-change experiments, and Arrhenius plots derived from the individual creep experiments. The former technique again involves the application of Equation 1 (this time at constant stress) and the same restrictions concerning stage II creep apply. The curves of the temperature-change experiments are shown in Fig. 4 and the calculated activation energies listed in Table II. An Arrhenius plot (log $\dot{\epsilon}$ versus $1/T$) for the individual creep runs is shown in Fig. 5 and the activation result included in Table II. An average value of activation energy of 140 kcal mol^{-1} resulted from the temperature-change experiments and 135 kcal mol^{-1} from the Arrhenius plot.

Transmission electron microscopic images of the structures before and after the creep tests are shown in Figs. 6 and 7. Voids and grain-boundary separation can be seen in the crept specimens. Such features might result from the ion-thinning process but their absence in the uncrept specimens and the fact that the specimen areas examined were selected away from the perforated areas of the foil preclude this explanation. These features, therefore, develop during creep and can be explained by the classic triple-point void formation accompanying grain-boundary sliding (Fig. 8). Also evident in this figure is dislocation activity in a grain in the vicinity of the void. This suggests that some plastic accommodation has also occurred in this case.

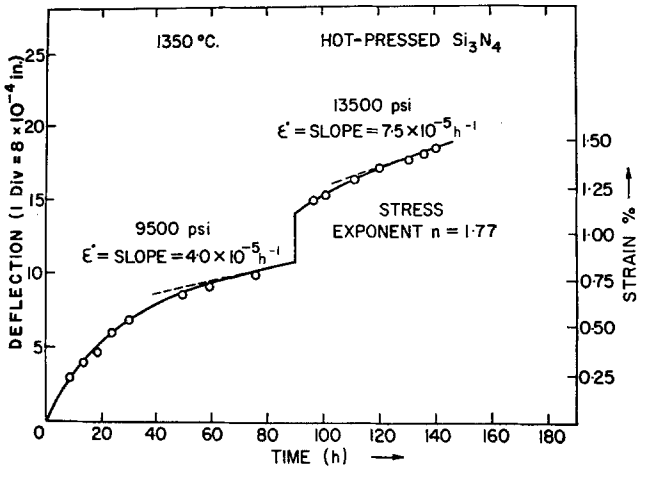

Figure 3 Stress-change data plot.

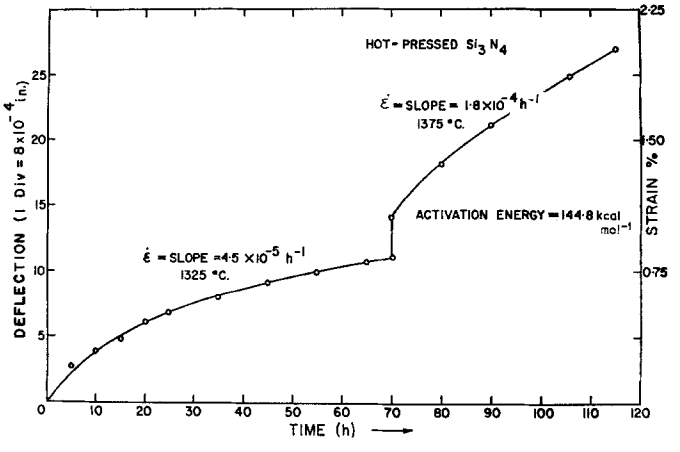

Figure 4 Temperature-change data plot.

4. Discussion

All the experimental creep curves exhibited the stage I transient and secondary stage II creep regimes. The third region, that of an accelerating creep rate, commonly observed in metals and some ceramic materials, was not attained within 250 h or a strain of $\sim$ 2.5%. To ensure the analysis of stage II creep, extended time tests were carried out.

The stress exponents ranged between 1.55 and 1.8. Purely viscous creep would give a stress exponent of 1. Hence, if grain-boundary sliding accommodated by a viscous mechanism were the rate-controlling mechanism, a value of n of 1 would be expected. A non-integral value of n has been obtained for other ceramic materials. Poteat and Yust [6] determined values of n between 1.04 and 1.59 for the creep of ThO_2; Passmore *et al.* [7] obtained $n = 1.5$ for the creep of ZrO_2 and Vasilos *et al.* [8] 1.60 for MgO. Gifkins [9] made a survey of the published creep data on a variety of materials and remarked that the non-integral value of n was due to the existence of "parallel-concurrent" mechanism of creep. Alden [10] and Heuer *et al.* [11] advanced the theory of non-Newtonian grain-boundary sliding involving climb-glide motion of dislocations near grain boundaries in fine-grain metallic systems and ceramic polycrystals. Fig. 1 indicates that there was no transition from one process to another over the range of stresses and temperatures employed. If it had taken place it would have been shown by two lines of different slopes instead of one continuous line. A non-Newtonian grain-boundary sliding model is the most likely explanation

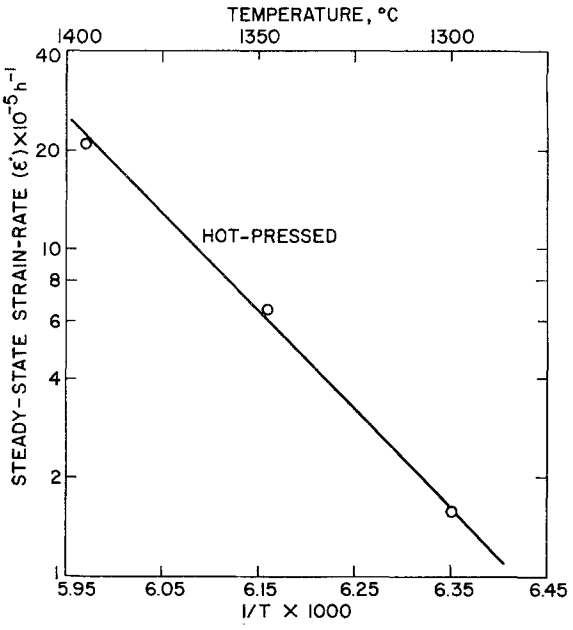

Figure 5 log $\dot{\epsilon}$ versus $1/T$ plot.

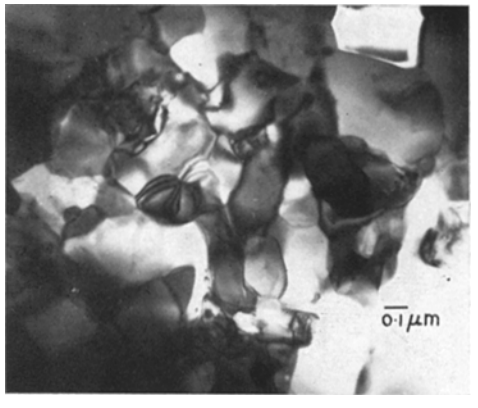

Figure 6 Microstructure of as-fabricated material.

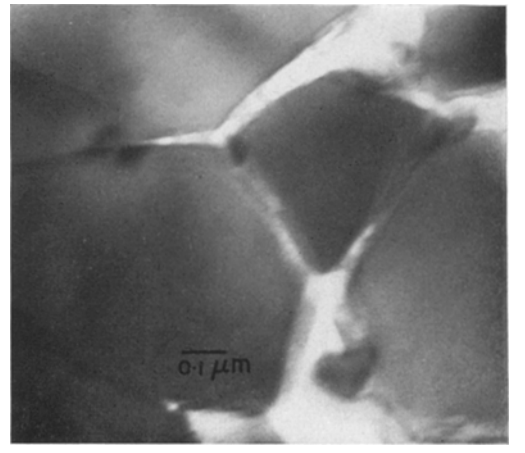

Figure 7 Grain-boundary separation after deformation.

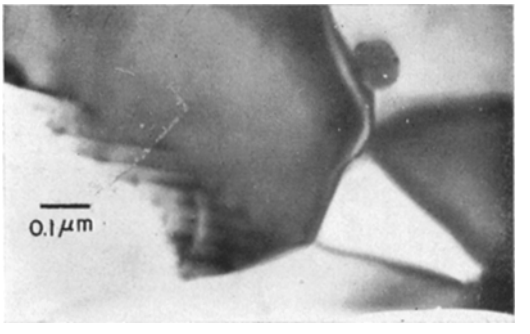

Figure 8 Void at triple point and grain-boundary dislocations.

of the creep results presently reported wherein creep occurs via the glassy grain-boundary phase (grain-boundary sliding) and accommodation mechanisms other than just void formation, such as localized plastic flow controlling the creep rate. The dislocation activity observed near some grain-boundary voids tends to support this explanation, and such "mixed" control could result in a non-integral stress exponent.

The activation energy in itself is not indicative of the creep mechanism but it is interesting to compare mechanisms suggested for some other ceramic materials having values of activation energies close to that determined in this work. Poteat and Yust [6] working on polycrystalline ThO_2 determined the activation energy for the creep process to be $\sim$ 120 kcal mol^{-1}. They observed voids and grain-boundary shearing following deformation. The activation energy for the creep of alumina was reported to be 126 $\pm$ 10 kcal mol^{-1} by Heuer *et al.* [11] and Sugita *et al.* [12] and in both cases, microstructural studies provided evidence of grain-boundary sliding accommodated by voids at triple points and associated grain-boundary dislocations. The activation energy for creep in the present work agrees with that reported by Kossowsky [13]. He observed triangular wedges to develop in

hot-pressed silicon nitride following creep and suggested grain-boundary sliding as the rate-controlling mechanism. However, the non-unity stress exponent value precludes grain-boundary sliding accommodated by viscous mechanism as exerting exclusive control of the creep rate, and a mixed control mechanism is suggested.

5. Conclusions

High temperature creep tests on hot-pressed silicon nitride showed that the creep rate was proportional to stress to ~ 1.7 power. Based on this value and microstructural observations of triple-point voids, and in some cases adjacent dislocation activity, a creep mechanism of grain-boundary sliding with some accommodation by dislocation climb and/or glide is suggested.

The activation energy for creep was calculated as 140 kcal mol^{-1} and this value compares favourably with other values obtained in ceramic systems in which grain-boundary sliding during creep has been observed.

Acknowledgement

The research for this paper was supported, in part, by The Defence Research Board of Canada, Grant number 7565-09, and samples were supplied by Norton Co.

References

1. E. GLENNY and T. A. TAYLOR, *Powder Met.* **8** (1961) 164.
2. R. F. STOKES, R. J. LUMBY and R. F. COE, *Abstract Bull. Amer. Ceram. Soc.* **51** (1972) 428.
3. WESTINGHOUSE RESEARCH LABORATORY, Pittsburgh, U.S.A., private communication.
4. S. TIMOSHENKO, "Strength of Materials, Part I, Elementary Theory and Problems" (Van Nostrand, New York, 1930) p. 359.
5. G. R. TERWILLIGER, Ph.D. Thesis, University of Utah, (1968) A-15.
6. L. E. POTEAT and C. E. YUST, *J. Amer. Ceram. Soc.* **49** (1966) 410.
7. E. M. PASSMORE, R. H. DUFF and T. VASILOS, *ibid* **11** (1966) 594.
8. T. VASILOS, J. B. MITCHELL and R. M. SPRIGGS, *ibid* **47** (1964) 203.
9. R. C. GIFKINS and K. U. SNOWDEN, *Trans. Met. Soc. AIME* **239** (1967) 910.
10. T. H. ALDEN, *Acta Met.* **15** (1967) 469.
11. A. H. HEUER, R. M. CANNON and N. J. TIGHE, in "Ultra fine-Grain Ceramics", edited by J. J. Burke, N. L. Reed and V. Weiss (Syracuse University Press, New York, 1970).
12. T. SUGITA and J. PASK, *J. Amer. Ceram. Soc.* **53** (1970) 609.
13. R. KOSSOWSKY, *J. Mater. Sci.* **8** (1973) 1803.

Received 22 November 1974 and accepted 8 January 1975.